EXPERIMENTAL AND NUMERICAL STUDIES ON BALLISTIC LAMINATES ON THE POLYETHYLENE AND POLYPROPYLENE MATRIX

P. Mayer*

Wroclaw University of Science and Technology
Faculty of Mechanical Engineering
Department of Foundry, Polymers and Automation
Laboratory of Plastics
Wroclaw, Poland

D. Pyka **K. Jamroziak**

Wroclaw University of Science and Technology
Faculty of Mechanical Engineering
Department of Mechanics, Materials Science and Engineering
Wroclaw, Poland

J. Pach

Wroclaw University of Science and Technology
Faculty of Mechanical Engineering
Department of Foundry, Polymers and Automation
Laboratory of Plastics
Wroclaw, Poland

M. Bocian

Wroclaw University of Science and Technology
Faculty of Mechanical Engineering
Department of Mechanics, Materials Science and Engineering
Wroclaw, Poland

ABSTRACT

The paper analyzes the issues relating to the applicability of innovative material systems for flexible composite armors. The authors made several samplings of aramid fibers (Kevlar 49) by replacing the epoxy resin base, which is often described in the literature, with the thermoplastic matrix - polyethylene (HDPE) and polypropylene (PP). The samples were fired with .38 Special Full Metal Jacketed (FMJ) ammunition produced by the S&B Company, and then the process of firing was modeled in the ABAQUS program. The advantages and disadvantages of the new material system including the possibility of its use in the construction of hybrid composite armors have been presented on the basis of the results of numerical analyses and ballistic tests.

Keywords: Composites, Polymers, Ballistic shields, Ballistic simulations.

1. INTRODUCTION

The terminal ballistics is the part of the ballistics as the science of projectile motion, with the focus on the description of the set of phenomena during the process of the mutual interaction between a projectile and a cover. It is a specific interaction, which consists of physical processes from the impact load until the penetration of a

* Corresponding author (paulina.mayer@pwr.edu.pl)

DOI : 10.1017/jmech.2017.103
Copyright © 2017 The Society of Theoretical and Applied Mechanics
https://doi.org/10.1017/jmech.2017.103 Published online by Cambridge University Press

projectile into a given cover. At the moment of the projectile impact, the kinetic energy is converted into deformation and the emission of the thermal energy of the projectile - cover system and the shock wave energy [1, 2]. Currently, composite materials have gained great popularity as components of ballistic shields. Especially those produced on the basis of high-strength fibers made artificially [3, 4]. Fibers that are the most commonly used as reinforcement in ballistic composites include: aramid fibers (Kevlar, Twaron, Rusar®, Teksar®), Ultra High Molecular Weight Polyethylene (UHMWPE) fibers (Dyneema®, Spectra®), glass and carbon fibers [5-8]. The PBO fibers (Zylon®) are less commonly used due to the low resistance to UV radiation [9], although in comparison with Kevlar they are characterized by higher energy absorption [10].

In addition to this type of reinforcement, the following factors have a decisive influence on the ballistic properties of a composite: its thickness, the sequence of the fabric layers arrangement (lay-up sequence), their connection to the matrix, and geometry [11-13]. The shape, weight, construction and kinetic energy of a projectile also affect the ballistic resistance of test materials. In the available literature on ballistic composites a lot of attention is given to experimental research that examines the aspect of the composite thickness [14, 15], the type of reinforcement [16, 17], nature of the damage [18, 19], perforation [20-22].

The matrix is another important factor determining the behavior of the composite during the impact. Chemically cured and thermoset materials boast a high degree of rigidity and brittle deformations occur during the impact. The use of the thermoplastic matrix in composites designed for ballistic shields is a better option by virtue of, among others, maximum deformation and pull-outs due to the weak adhesion between fibers and the matrix [23], the increased dissipation energy resulting from delamination and debonding [24, 25]. Gopinath *et al*., in their work described the influence of selected flexible and rigid matrices on the ballistic properties of lightweight protection armors. The finite element method allowed for the performance of, among others, simulations of armors with the use of materials without a matrix and with two differing matrices, with the application of the LS-DYNA program. The conducted analysis of the impact of a projectile on the armor made it possible to characterize the size and type of occurring deformations. It has been found that the matrix in composite materials reduces the maximum deflection of the armor, increases the size of the deformed area as well as the kinetic energy of a projectile [26].

Composites with the fibers mentioned above are characterized by several properties, which make them ideal for the application on ballistic shields. They have a low weight, a programmable structure, high specific strength and high capacity to absorb the ballistic impact energy. For this reason, these materials are commonly used to perform light panels of military and civilian vehicles [27, 28], bulletproof vests [29] and helmets [30, 31].

In view of the ongoing development of composite materials, the new solutions are sought to improve the protection of people against adverse effects of weapons. The authors of numerous works taking up the widely understood theme of materials used in ballistics have been examining their different aspects influencing the impact properties.

The authors of [32] studied the composite armors reinforced with aramid fabric (Kevlar 29) on the thermoset matrix. Ballistic tests were carried out for laminates containing 8, 10, 13 and 15 layers of fabrics of plain weave. The thickness of the received laminates was subsequently: 4.3; 5.3; 7 and 8 mm. The results of the numerical analysis differed only by 8% from experimental studies of the received laminates. Kulkarni *et al*. in the work [33] also tested ballistic properties of composites with aramid fabric, which contained an additional layer of an aluminum alloy. In the composites based on epoxy resin, obtained by using hand lay-up technique, there were analyzed: dissipation energy, deformation, perforation, a type of damage caused after firing a projectile at the impact velocity of 871 m/s and the impact energy of 3687 J. Apart from strengthening laminates with additional metallic layers, the authors of the publication [34] produced epoxy-glass laminates with nano clay of 1-5 wt. % of matrix. In addition to the experimental studies there was carried out the numerical analysis, which took into account the energy absorption caused by tensile failure of primary fibers, deformation of secondary fibers, and matrix delamination crack. The authors of [35] undertook impact tests at two different velocities and diameters of a projectile. Laminates made from the sewn graphite fabric on the epoxy matrix were the subject of investigations. As foreseen by the authors, the energy of perforation increased with extending the thickness of the laminate and the projectile diameter.

Following a review of the existing literature, the authors of this study concluded that the use of the thermoplastic matrix can affect more favorably the impact resistance of composites used as lightweight ballistic shields rather than the use of thermoset or chemically cured materials. The authors particularly focused on the research of ballistic laminates prepared on the polypropylene and polyethylene matrix and aramid fabric.

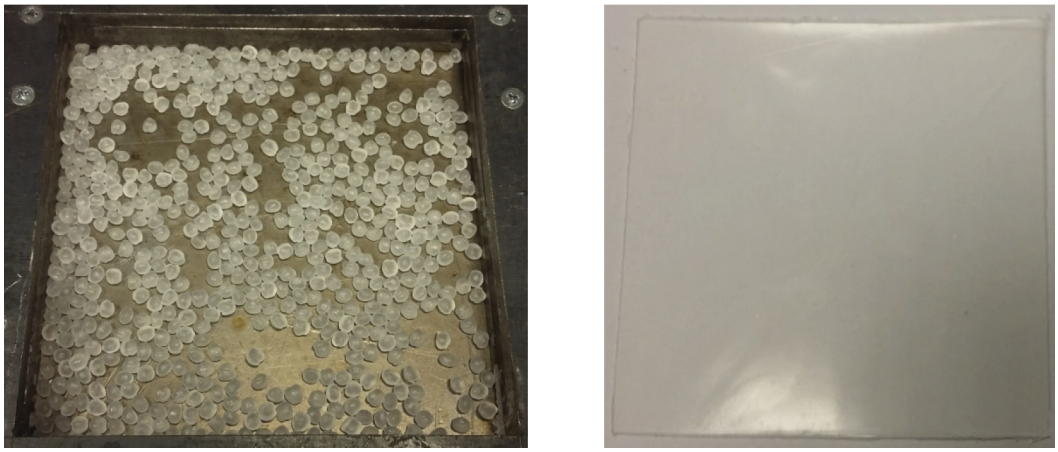
2. EXPERIMENTAL WORK

2.1 Material and Specimens

The following thermoplastic polymers: the high-density polyethylene (HDPE), trade name Hostalen ACP 9255 Plus, and the polypropylene (PP) Moplen HP548R produced by LyondellBasell were applied as the matrices of the laminates tested in the work. The aramid fabric Kevlar 49 constituted the reinforcement.

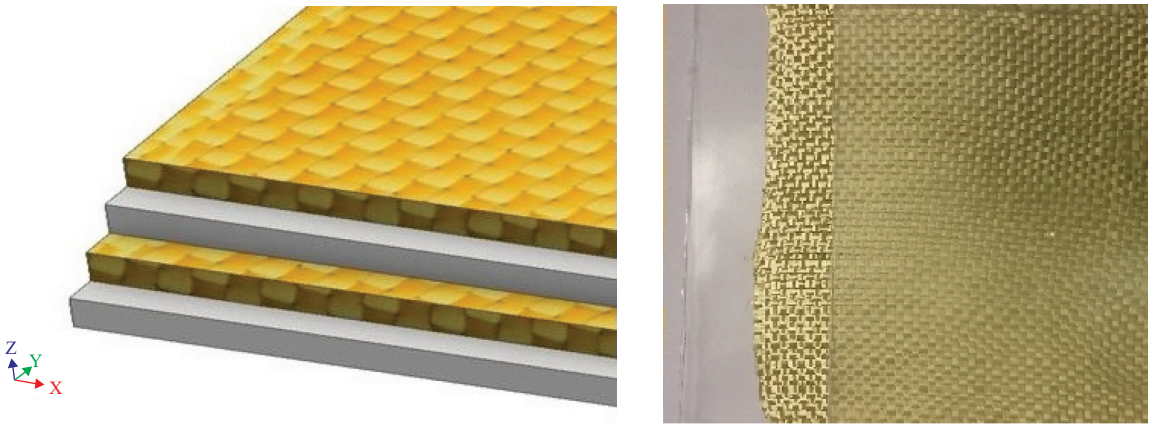
The laminates were formed in two stages. The first step was the formation of the polymer film from granulate which initially was plasticized under a press at the temperature of 200°C for 2 min. without load, and then for 2 min. under the pressure of 2 MPa. As a result of pressing, approximately 500 micron thick polymer films

https://doi.org/10.1017/jmech.2017.103 Published online by Cambridge University Press



(a) (b)

Fig. 1 Forming of the laminate polymer layer: (a) the polymer in the form of granulate, before heat-processing, (b) the formed polymer film.



(a) (b)

Fig. 2 The laminate layering: (a) visualization, (b) the real image.

were obtained (Fig. 1).

The laminates were produced by the alternate pressing of 11 layers of polymer film and 10 layers of aramid fabric arranged in a metal mold. The layering is presented in Fig. 2. The laminates were molded at the temperature of 200°C. They were pressed for 2 min. with no load and for 3 min. under the pressure of 5 MPa. The work stand for laminate forming is shown in Fig. 3.

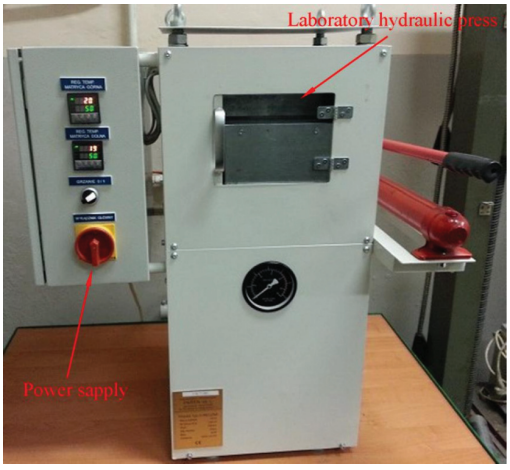


Fig. 3 The work stand for producing thermoplastic laminates.

2.2 Formulation of the Problem

The estimation of the energy dissipation of the projectile can be expressed by the approximation of physical-mathematical relations to the real phenomena occurring when the projectile impacts the shield (Fig. 4). If inside an object (laminate) there is separated a base element of a predetermined area ΔS and the normal n, to which the resultant force ΔP is applied, the stress vector can be defined at such a point as:

$$P = \lim_{\Delta S \to 0} \frac{\Delta P}{\Delta S} = \frac{dP}{dS} \tag{1}$$

The displacement of the points of the deformed body can be described by introducing a displacement vector u,

https://doi.org/10.1017/jmech.2017.103 Published online by Cambridge University Press

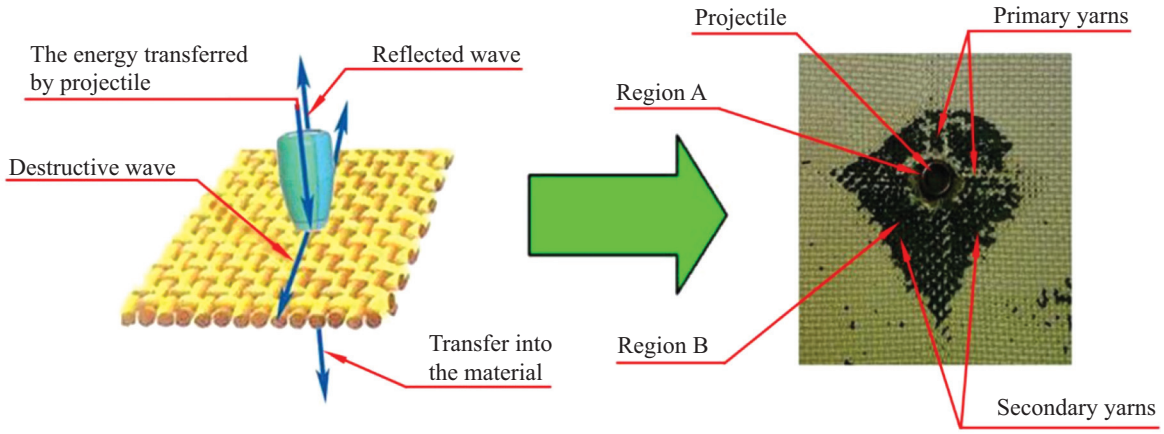


Fig. 4 The scheme of physical relations affecting the destruction of the laminate layers resulting from the ballistic impact.

which can be written for the general coordinate system (x, y, z):

$$u = u(u_1, u_2, u_3) \tag{2}$$

and each component is the function of displacement and time

$$u_i = u_i(x, y, z, t) \tag{3}$$

The Euler strain tensor can be written as:

$$e_{ij} = \frac{1}{2}(u_{ij} + u_{ji} - u_{mi} \cdot u_{mj}) \tag{4}$$

The tensor $e_{ij} = \frac{1}{2}(u_{ij} + u_{ji})$ is called the small strain tensor. The strain intensity is defined as:

$$\varepsilon_e = \sqrt{\frac{2}{3}\varepsilon_{ij}\varepsilon_{ji}} \tag{5}$$

The hypothesis on the member function F, zeroing at the edges of the area corresponding to an elastic state, can be written as:

$$F = F(\sigma_{ij}, \varepsilon_{ij}^p, k) \tag{6}$$

where:

σ_{ij} – components of the stress tensor,

ε_{ij}^p – components of the tensor of elastic strains,

k – the functional depending on state of stress and strain.

The Huber-Mises-Hencky yield criterion is applied to determine the function F (6), under which the transition into the elastic state is determined by the strain energy of volume change, and thus the second invariant of the stress tensor deviator expressed as:

$$F = J_{2S} - \frac{1}{3}Y^2 = \frac{1}{3}S_{ij} \cdot S_{ji} - \frac{1}{3}Y^2 = 0 \tag{7}$$

where:

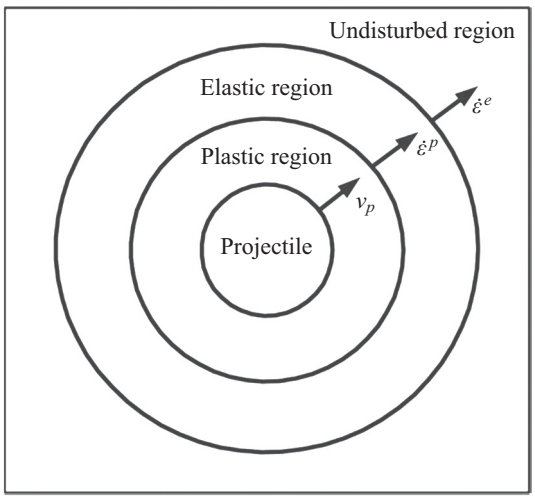


Fig. 5 A schematic illustration of elastic and plastic compression zones at the section of penetrating into soil looking in the direction of penetration.

J_{2S} – the invariant of the stress tensor,

Y – the function of Johnson-Cook (J-C) model,

S_{ij} – the stress tensor deviator.

While in Johnson-Cook model it is assumed that the function Y is defined as:

$$Y = [A + B(\varepsilon^p)^n](1 + C \ln \dot{\varepsilon}_*^p)[1 - (T_*)^m] \tag{8}$$

where:

A, B, C, n, m – empirical parameters,

$\dot{\varepsilon}_*^p, T_*$ – standardized values of strain intensity changes in terms of the elastic strain ratio and temperature.

Therefore, on the basis of the mathematical analysis, the phenomenon of shield strain can be reduced to local issues in terms of destructive strains, plastic strains, elastic strains and the undisturbed region (Fig. 5).

https://doi.org/10.1017/jmech.2017.103 Published online by Cambridge University Press

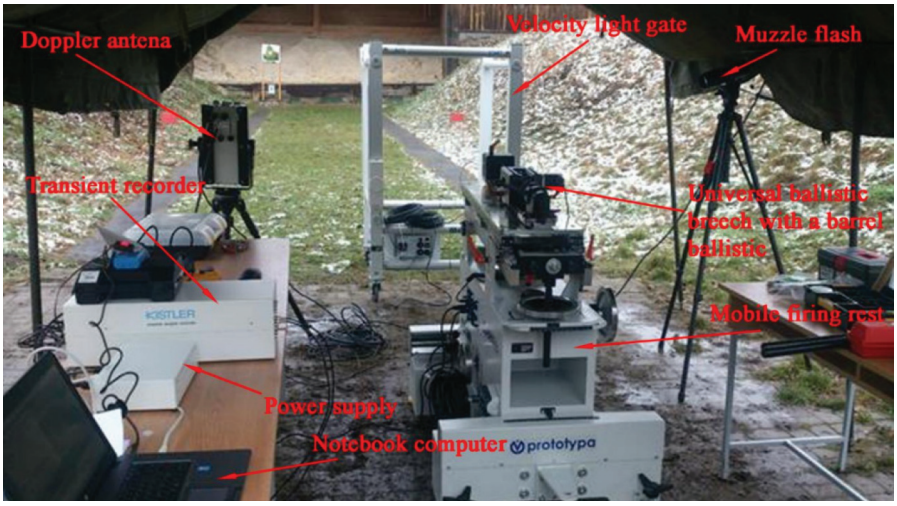


Fig. 6 Components of the ballistic test stand.



(a) (b)

Fig. 7 The projectile of .38 Special of the FMJ type to fire samples: (a) a projectile, (b) a deformed projectile.

2.3 Methodology of Ballistic Tests

The samples were fired on the ballistic track with the use of the position with the ballistic barrel UZ 2002 produced by PROTOTYPA-ZM, according to the European Norm CEN EN 1522. Velocities were measured by the Doppler radar type Weibel SL-525PE. The position of the ballistic tests is shown in Fig. 6. Three consecutive shots were given to each sample. The projectile with a lead core (Fig. 7), the weight of 10.25 g and the initial velocity showed in Table 1.

As a result of firing samples that were rigidly attached to holders without support it was found that, unlike the laminates on the polyethylene matrix, the laminates of the polypropylene matrix stopped the projectile. The view of the samples after firing is presented in Figs. 8 and 9 respectively.

As shown in Fig. 8, the sample with the PP matrix stopped the projectile, and its deflection reached 11 mm. Figure 8(b) presents the shearing of aramid fibers. The laminate was partly punctured (Fig. 8(c)), which refers to several laminates, but the projectile did not pass through the sample. In contrast to the laminates on the epoxy matrix, described in the literature [33, 34], no participation of virgin fibers in the sample deformation was observed in the polypropylene laminates. The polypropylene matrix was detached from the aramid fabric. Additionally, there was observed the destruction of the laminate virgin fibers and their pull-out of the initially arranged fabric. The brittle fracture of the matrix and shearing fibers in the first layers of the aramid fabric is clearly seen. The incomplete lamination of aramid fabric, the lack of saturation of individual fibers exerted a positive influence on the free operation of the individual layers, as evidenced by the projectile strain. In the sample with the PE matrix (see Fig. 9(b)), the destruction mechanism concentrates mostly of primary fibers that are pulled out of the weave of the fabric and then cut (Fig. 9(c)). This mechanism of damage the sample after firing corresponds to a projectile deformation.

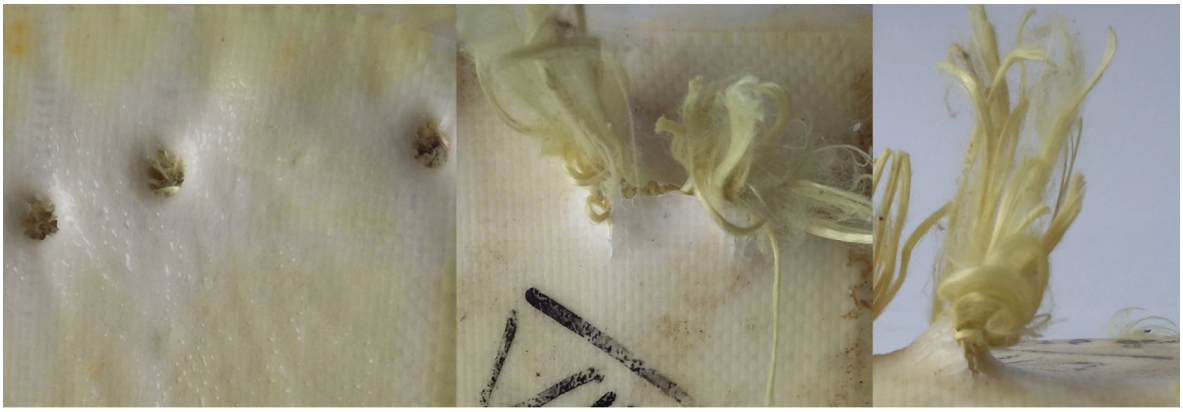
The results of deformation obtained in the samples with the PP matrix and the PE matrix are different (Fig.

https://doi.org/10.1017/jmech.2017.103 Published online by Cambridge University Press



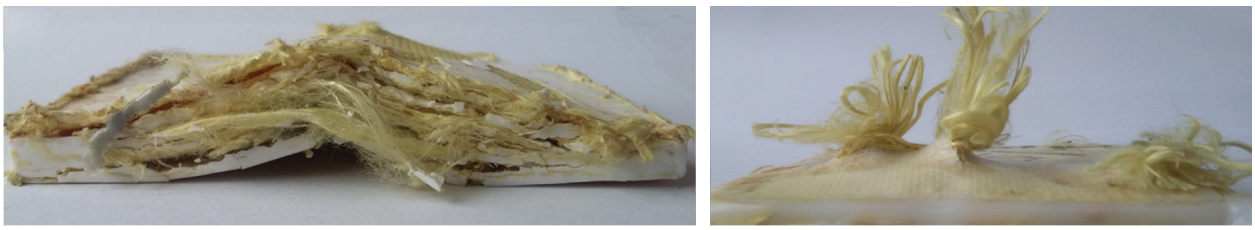
(a) (b) (c)

Fig. 8 The laminate with aramid fibers on the polypropylene matrix after firing: (a) a view of the sample from the side of the projectile impact, (b) the zoomed damaged area, (c) the effect of damage from the side of the projectile exit.



(a) (b) (c)

Fig. 9 The laminate with aramid fibers on the polyethylene matrix after firing: (a) a view of the sample from the side of the projectile impact, (b) the effect of damage from the side of the projectile exit, (c) the view of the destruction area with characteristic pulled out virgin fibers.



(a) (b)

Fig. 10 Deformations the laminates: (a) on the polypropylene matrix, (b) on the polyethylene matrix.

10), referring to their effects on the literature [36] in which the PP laminates were studied. However, direct comparisons are not possible due to the different architectures of fabric used and other type of bullets with different projectile shape [37, 38] and range of outlet velocity (260-270 m/s). In addition the projectiles deformations are slightly different.

The view of projectiles, deformed after having the shields struck, is shown in Fig. 11.

The strain of the projectiles No. 1 and 2 resulted from firing the sample on the polypropylene matrix, the projectiles No. 3 and 4 were deformed after firing the laminate on the polyethylene matrix. Deformation projectiles No. 1 and 2 in their frontal surface are more flattened than No. 3 and 4. Front surfaces of projectiles No. 3 and 4 are similar to the convex (mushroom) shape. The stopped projectile in the PP laminate (where the residual velocity was 0 m/s) absorbed more of the impact energy, as a result of the fact that the projectile was more deformed. On the other hand, the projectile shot in the PE sample passed through it, as was evidenced by the recorded residual velocities.

https://doi.org/10.1017/jmech.2017.103 Published online by Cambridge University Press



Fig. 11 38 projectiles strained after striking the studied shields.

Table 1 Recorded velocity after shooting in the laminates.

Sample	PP 1	PP 2	PP 3	PE 1	PE 2	PE 3
Initial velocity [m/s]	256	266	267	258	263	259
Residual velocity [m/s]	0	0	0	47	65	75
Effect of shooting	stopped	stopped	perforation (projetile was stopped by primary fibers) (Fig. 8(c))	perforation	perforation	perforation

2.4 Numerical Analysis

The strain of laminates was also verified by the finite element method for the purpose of enabling the mathematical description (see part 3) of physical relations occurring at the interface of the projectile –the shield. The numerical analysis was performed in the ABAQUS environment, preceded by the thorough literature review [39-44]. Aramid laminates on the polymer matrix were modeled as layered elements with visible separation of individual layers. Tables 2 and 3 summarize material properties of the projectile and the laminates made of aramid fabric and thermoplastic polymers analyzed in the work. The modeling of the projectile jacket was abandoned after initial simulations due to its negligible share in the process under consideration, as the core of a projectile is a decisive factor. Similarly, it was noted that the rotational velocity of the projectile as a component of the total impact energy does not significantly affect the destruction of shields, which has been considered in [39]. The Johnson-Cook constitutive equation with destruction was applied for all models [45-49].

For the work purposes there were performed simulations of the projectile deformation after the impact on the aramid laminates on two thermoplastic matrices. The actual averaged velocity of the projectile was of 263 m/s, under simulation conditions the velocity set-point was similar to v_1, i.e. 250 m/s. The mass of the projectile adopted to the numerical analysis was 10.25 g. The restraint of the projectile was blocked at the two side edges where $Ux = Uy = Uz = \alpha x = \alpha y = \alpha z = 0$, where Ux, Uy, Uz – translations (x, y, z), and αx, αy, αz – rotations (x, y, z).

The numerical simulations allowed for the achievement of the following courses of the projectile deformation (Fig. 12), and general imaging of the strain of the analyzed ballistic shield on the example of the results obtained from the ballistic experiment. The summary is depicted in Fig. 13. As shown in the experiment, the deformation area in Fig. 13(b) (damage of the PP matrix) is similar to the gray area obtained in the simulations (Fig. 13(a)). Presented areas in the local view have a high degree of similarity model assumptions and therefore the J-C has been defined correctly.

Another equally important element of the correctness of the conducted simulations was the verification of the phase diagrams for the impact velocity of the projectile and for the absorption of the kinetic energy by the system projectile - shield. The example below (Fig. 14) is given for the sample of the PP type and the shot No. 1, where the measured velocity was similar to the velocity adopted in the simulation.

https://doi.org/10.1017/jmech.2017.103 Published online by Cambridge University Press

Table 2 Material properties of the projectile [50].

Core: lead alloy Pb1 with antimony					
E [GPa]	v [-]	ρ [kg/m^3]	A [MPa]	B [MPa]	n [-]
1.3	0.42	11300	5.1	35	0.5
Jacket: Brass M90 PN-92/H-87025					
130	0.375	8940.9	112	505	0.42

Table 3 Material properties of the shield [51].

Kevlar 49							
E [GPa]	v [-]	ρ [kg/m^3]	A [MPa]	B [MPa]	n [-]	$SIGY$ [N/m^2]	FS [-]
90	0.3	1440	-	-	-	3.6e+9	0.04
Polypropylene (PP)							
1.5-2.5	0.45	900	20 -38	8-12	0.15	-	-
Polyethylene (PEHD)							
0.6-1.4	0.46	960	40	25	0.18	-	-

E - Young's modulus, v - Poisson's ratio, A - Yield at zero plastic strain, B - Hardening constant, n - Hardening exponent, $SIGY$ - Yield strength, FS - Effective plastic strain, failure criterion

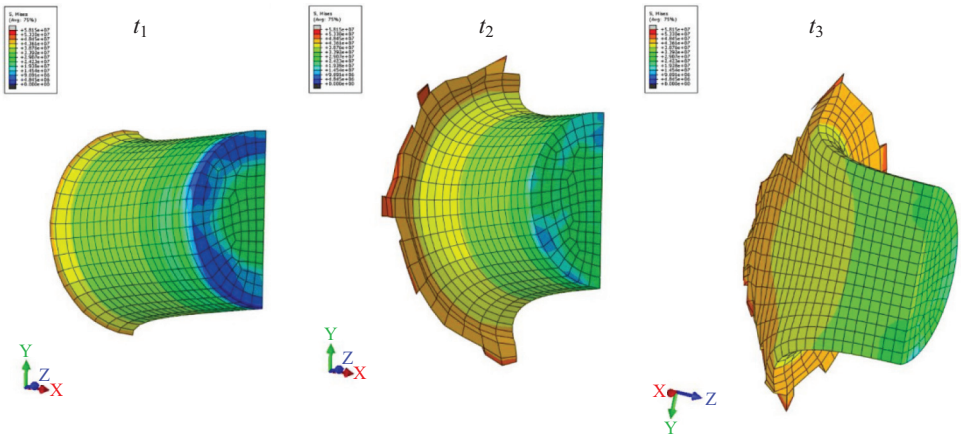
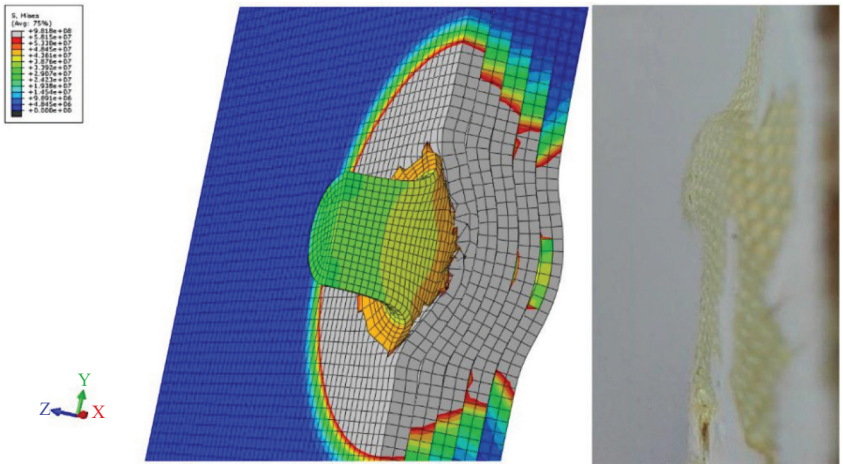


Fig. 12 Deformations of the lead core of the projectile .38 for the times: $t_1 = 5.0 \times 10^{-5}$ s, $t_2 = 12.5 \times 10^{-5}$ s, $t_3 = 2.0 \times 10^{-4}$ s.



(a) (b)

Fig. 13 The comparison of experimental results with the numerical analysis: (a) the numerical simulation for the time tend = 2.5×10^{-4} s, (b) the result of the damaged PP shield.

https://doi.org/10.1017/jmech.2017.103 Published online by Cambridge University Press

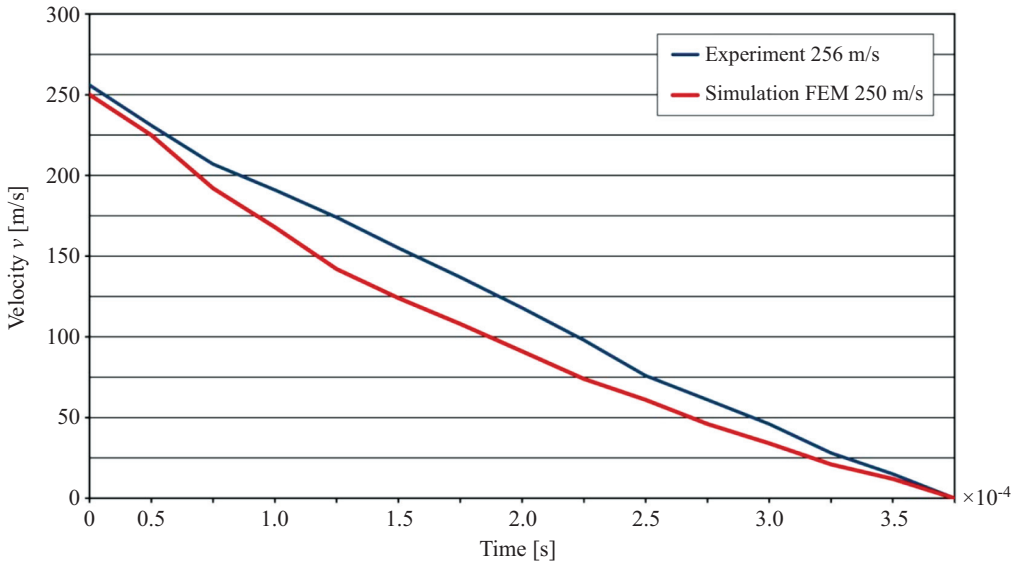


Fig. 14 The diagram of the projectile velocity as the function of time.

3. CONCLUSIONS

Based on the studies carried out, the authors concluded that the shield with the polypropylene matrix had higher resistance to the ballistic impact than the polyethylene matrix. Both of the laminates analyzed in the work were of similar, relatively small own weight of 55 g for samples on the polypropylene matrix and of 67 g for samples on polyethylene matrix.

The laminates on the polypropylene matrix demonstrated the ballistic efficiency by stopping the .38 Special FMJ projectile produced by S&B. Aramid fibers in these samples got sheared at the initial stage as seen in Fig. 8. In the laminates on the polyethylene matrix the fibers were pulled out of the fabric upon impact of the projectile (Fig. 9), which may prove the insufficient adhesion between the aramid fibers and the polymer.

The numerical modeling of the system *projectile - shield* significantly enhanced the analysis of the energy absorption of the bullet impact. It was proved that the assumed mathematical formulae in the J-C model were correctly defined for the newly designed laminate shield, which confirms the validity of the undertaken work (Figs. 13-14). In the authors' subjective assessment the treatment of the projectile jacket as a whole with a core gives results similar to those obtained from experimental studies. Nevertheless, such solutions should be sought to accurately reproduce the estimation of the effect of energy dissipation. The percentage of the kinetic energy responsible for the deformation of components of particular elements of the projectile and components of the shield structure can be specified only by numerical investigations supported by selected material studies. Such knowledge will enable the optimal design of shields, which the authors intend to continue in further studies.

To sum up, the proposal to use the laminates on the polypropylene matrix is some kind of alternative to other materials of the matrix. In this case, the achieved mass parameters were slightly better than for the standard shields with epoxy matrices. However, it is necessary to verify other factors, such as aging, as it is generally known that traditional matrices are sensitive to the operational environment and require specific treatments in terms of the protective coating application.

REFERENCES

1. Abrate, S., *Impact on Composite Structures*, Cambridge University Press, Cambridge (1998).
2. Carlucci, D. E. and Jacobson, S. S., *Ballistic. Theory and Design of Guns and Ammunition*, Taylor & Francis Group, LLC, Boca Raton (2008).
3. Reid, S. R. and Zhou, G. (ed), *Impact Behaviour of Fibre-Reinforced Composite Materials and Structures*, Woodhead Publishing Limited and CRC Press LLC, Boca Raton (2008).
4. Rojek, M. *et al*., "Composite Materials with the Polymeric Matrix Applied to Ballistic Shields," *Archives of Materials Science and Engineering*, **63**, pp. 26-35 (2013).
5. Gogineni, S., Gao, X. L., David, N. V. and Zheng, J. Q., "Ballistic Impact of Twaron CT709 Plain Weave Fabrics," *Mechanics of Advanced Materials and Structures*, **19**, pp. 441-452 (2012).
6. Sapozhnikov, S. B., Kudryavtsev, O. A. and Zhikharev, M. V., "Fragment Ballistic Performance of Homogenous and Hybrid Thermoplastic Composites," *International Journal of Impact Engineering*, **81**, pp. 8-16 (2015).
7. Hazzard, M. K., Hallett, S., Curtis, P. T., Iannucci, L. and Trask, R. S., "Effect of Fibre Orientation on the Low Velocity Impact Response of Thin Dyneema Composite Laminates," *International Journal of*

https://doi.org/10.1017/jmech.2017.103 Published online by Cambridge University Press

Impact Engineering, **100**, pp. 35-45 (2016).

8. Nguyen, L. H. *et al*., "A Methodology for Hydrocode Analysis of Ultra-High Molecular Weight Polyethylene Composite under Ballistic Impact," *Composites: Part A*, **84**, pp. 224-235 (2016).
9. Wesolowska, M. and Delczyk-Olejniczak, B., "The Fibers in Ballistics- Today and Tomorrow," *Technical Textiles*, pp. 41-50 (2011).
10. Pereira, M. J. and Revilock, D. M., "Ballistic Impact Response of Kevlar 49 and Zylon under Conditions Representing Jet Engine Fan Containment," *Journal of Aerospace Engineering*, **22**, pp. 240-248 (2009).
11. Cheeseman, B. A. and Bogetti, T. A., "Ballistic Impact into Fabric and Compliant Composite Laminates," *Composite Structures*, **61**, pp. 161-173 (2003).
12. Pandya, K. S., Dharmane, L., Pothnis, J. R., Ravikumar, G. and Naik, N. K., "Stress Wave Attenuation in Composites during Ballistic Impact," *Polymer Testing,* **31**, pp. 261-26 (2012).
13. García-Castillo, S. K., Sánchez-Sáez, S. and Barbero, E., "Nondimensional Analysis of Ballistic Impact on Thin Woven Laminate Plates," *International Journal of Impact Engineering*, **39**, pp. 8-15 (2012).
14. Gellert, E. P., Cimpoeru, S. J. and Woodward, R. L., "A Study of the Effect of Target Thickness on the Ballistic Perforation of Glass-Fibre-Reinforced Plastic Composites," *International Journal of Impact Engineering*, **24**, pp. 445-456 (2000).
15. Caprino, G., Lopresto, V. and Santoro, D., "Ballistic Impact Behaviour of Stitched Graphite/Epoxy Laminates," *Composites Science and Technology*, **67**, pp. 325-335 (2007).
16. Cork, C. R. and Foster, P. W., "The Ballistic Performance of Narrow Fabrics," *International Journal of Impact Engineering*, **34**, pp. 495-508 (2007).
17. Kedzierski, P., Gieleta, R., Morka, A., Niezgoda, T. and Surma, Z., "Experimental Study of Hybrid Soft Ballistic Structures," *Composite Structures*, **153**, pp. 204-211 (2016).
18. Nunes, L. M., Paciornik, S. and D'almeida, J. R. M., "Evaluation of the Damaged Area of Glass-Fiber-Reinforced Epoxy-Matrix Composite Materials Submitted to Ballistic Impacts," *Composites Science and Technology*, **64**, pp. 945-954 (2004).
19. Boccaccini, A. R., Atiq, S., Boccaccini, D. N., Dlouhy, I. and Kaya, C., "Fracture Behaviour of Mullite Fibre Reinforced–Mullite Matrix Composites under Quasi-Static and Ballistic Impact Loading," *Composites Science and Technology*, **65**, pp. 325-333 (2005).
20. Sheikh, A. H., Bull, P. H. and Kepler, J. A., "Behaviour of Multiple Composite Plates Subjected to Ballistic Impact," *Composites Science and Technology*, **69**, pp. 704-710 (2009).
21. Hirai, Y., Hamada, H. and Kim, J. K., "Impact Response of Woven Glass-Fabric Composites- I. Effect of Fibre Surface Treatment," *Composites Science and Technology*, **58**, pp. 91-104 (1998).
22. Sabet, A. R., Beheshty, M. H. and Rahimi, H., "Experimental Study of Sharp-Tipped Projectile Perforation of GFRP Plates Containing Sand Filler under High Velocity Impact and Quasi-Static Loadings," *Polymer Composites*, **30**, pp. 1497-1509 (2009).
23. Cheeseman, B. A. and Bogetti, T. A., "Ballistic Impact into Fabric and Compliant Composite Laminates," *Composite Structures*, **6**, pp. 161-173 (2003).
24. Carrillo, J. G., Gamboa, R. A., Flores-Johnson, E. A. and Gonzalez-Chi, P. I., "Ballistic Performance of Thermoplastic Composite Laminates Made from Aramid Woven Fabric and Polypropylene Matrix," *Polymer Testing*, **3**, pp. 12-519 (2012).
25. Iremonger, M. J. and Went, A. C., "Ballistic Impact of Fibre Composite Armours by Fragment-Simulating Projectiles," *Composites Part A*, **27A**, pp. 575-581 (1996).
26. Gopinath, G., Zheng, J. Q. and Batra, R. C., "Effect of Matrix on Ballistic Performance of Soft Body Armor," *Composite Structures*, **94**, pp. 2690-2696 (2012).
27. Gower, H. L., Cronin, D. S. and Plumtree, A., "Ballistic Impact Response of Laminated Composite Panels," *International Journal of Impact Engineering*, **35**, pp. 1000-1008 (2008).
28. Awoukeng-Goumtcha, A., Taddei, L., Tostain, F. and Roth, S., "Investigations of Impact Biomechanics for Penetrating Ballistic Cases," *Bio-Medical Materials and Engineering*, **24**, pp. 2331-2339 (2014).
29. Yang, Y. and Chen, X., "Study of Energy Absorption and Failure Modes of Constituent Layers in Body Armour Panels," *Composites Part B*, **98**, pp. 250-259 (2016).
30. Kulkarni, S. G., Gao, X. L., Horner, S. E., Zheng, J. Q. and David, N. V., "Ballistic Helmets – Their Design, Materials, and Performance against Traumatic Brain Injury," *Composite Structures*, **101**, pp. 313-331 (2013).
31. Tham, C. Y., Tan, V. B. C. and Lee, H. P., "Ballistic Impact of a KEVLAR Helmet: Experiment and Simulations," *International Journal of Impact Engineering*, **35**, pp. 304-318 (2008).
32. Sorrentinoa, L., Bellinia, C., Corradoa, A., Polinia, W. and Aricòb, R., "Ballistic Performance Evaluation of Composite Laminates in Kevlar 29," *Procedia Engineering*, **88**, pp. 255-262 (2015).
33. Haro, E. E., Akindele, G. O. and Szpunar, J. A., "The Energy Absorption Behavior of Hybrid Composite Laminates Containing Nano-Fillers under Ballistic Impact," *International Journal of Impact Engineering*, **96**, pp. 11-22 (2016).
34. Balaganesan, G., Velmurugan, R., Srinivasan, M., Gupta, N. K. and Kanny, K., "Energy Absorption

https://doi.org/10.1017/jmech.2017.103 Published online by Cambridge University Press

and Ballistic Limit of Nanocomposite Laminates Subjected to Impact Loading," *International Journal of Impact Engineering*, **74**, pp. 57-66 (2014).

35. Caprino, G., Lopresto, V. and Santor, O. D., "Ballistic Impact Behaviour of Stitched Graphite/Epoxy Laminates," *Composites Science and Technology*, **67**, pp. 325-335 (2007).
36. Bandaru, A. K., Chavan, V. V., Ahmad, S., Alagirusamy, R. and Bhatnagar, N., "Ballistic Impact Response of Kevlar® Reinforced Thermoplastic Composite Aarmors," *International Journal of Impact Engineering*, **89**, pp. 1-13 (2016).
37. Bandaru, A. K. and Ahmad, S., "Effect of Projectile Geometry on the Deformation Behavior of Kevlar Composite Armors under Ballistic Impact," *International Journal of Applied Mechanics*, **7**, 1550039 (2015).
38. Ben-Dor, G., Dubinsky, A. and Elperin, T., *Applied High-Speed Plate Penetration Dynamics,* Springer, Berlin (2006).
39. Bocian, M., Jamroziak, K. and Kosobudzki, M., "Analysis of Material Punching Including a Rotational Speed of the Projectile," *Solid State Phenomena*, **220-221**, pp. 571-576 (2015).
40. Rusinski, E., Karlinski, J. and Jamroziak, K., "The Chosen Aspects from Research of Ballistic Shields," *Proceedings of the 22nd DANUBIA-ADRIA Symposium on Experimental Methods in Solid Mechanics DAS*, Monticelli Terme-Parma, Italy (2005).
41. Kedzierski, P., Poplawski, A., Gieleta, R. and Slawinski, G., "Experimental and Numerical Investigation of Fabric Impact behavior," *Composites Engineering Part B*, **69**, pp. 452-459 (2015).
42. Pyka, D., Jamroziak, K., Blazejewski, W. and Bocian, M., "Calculations with the Finite Element Method during the Design Ballistic Armour," *Proceedings of the 13th International Scientific Conference, Computer Aided Engineering*, Rusinski E., Pietrusiak D. (eds), Springer International Publishing AG, pp. 451-459 (2017).
43. Stanislawek, S., Morka, A. and Niezgoda, T., "Pyramidal Ceramic Armor Ability to Defeat Projectile Threat by Changing its Trajectory," *Bulletin of the Polish Academy of Sciences, Technica Sciences*, **63**, pp. 843-849 (2015).
44. Yahaya, R., Sapuan, S. M., Jawaid, M., Leman, Z. and Zainudin, E. S., "Measurement of Ballistic Impact Properties of Woven Kenaf-Aramid Hybrid Composites," *Measurement*, **77**, pp. 335-343 (2016).
45. Lim, C. T., Shim, V. P. W. and Ng, Y. H., "Finite-Element Modeling of the Ballistic Impact of Fabric Armor," *International Journal of Impact Engineering*, **28**, pp. 13-31 (2003).
46. Malachowski, J., *Influence of HE Location on Elastic-Plastic Tube Response under Blast Loading, Shell Structures Theory and Applications*, Taylor & Francis Group, London, **2**, pp. 179-182 (2010).
47. Shim, V. P. W., Tan, V. B. C. and Tay, T. E., "Modelling Deformation and Damage Characteristics of Woven Fabric under Small Projectile Impact," *International Journal Impact Engineering*, **16**, pp. 585-605 (1995).
48. Panowicz, R. and Janiszewski, J. "Tensile Split Hopkinson Bar Technique: Numerical Analysis of the Problem of Wave Disturbance and Specimen Geometry Selection," *Metrology and Measurement Systems*, **23**, pp. 425-436 (2016).
49. Grujicic, M., Arakere, G., Gogulapati, M. and Cheeseman, B. A., "A Numerical Investigation of the Influence of Yarn-Level Finite-Element Model on Energy Absorption by a Flexible-Fabric Armour during Ballistic Impact," *Proceedings of the Institution of Mechanical Engineers, Part L: Journal of Materials: Design and Applications,* **222**, pp. 259-276 (2008).
50. Jamroziak, K. *et al., Impact Resistance of Ballistic Shields of Personal Protection in Relation to Selected Small Arms Ammunition, an Unpublished Report Part 1*, Military Academy of Land Forces, Wroclaw (2005) (in Polish).
51. Jamroziak, K., *An Identification of the Material Properties in the Terminal Ballistic*, Wroclaw University of Technology Publishing House, Wroclaw (2013).

(Manuscript received May 30, 2017,
accepted for publication September 8, 2017.)

https://doi.org/10.1017/jmech.2017.103 Published online by Cambridge University Press